

Mechanical, Structural and Catalytic Properties of the Co-Al-O Coatings

Kazys BABILIUS, Artūras BABILIUS*

Department of Manufacturing Technologies, Kaunas University of Technology, Kęstučio 27, LT-44025 Kaunas, Lithuania

Received 25 March 2009; accepted 05 March 2010

Co-Al-O type nanocrystalline catalytic coatings of 30 μm thickness were formed by the activated thermo-chemical condensate deposition (AT-CCD) method on the strip steel 0C-404 of 40 μm thickness. After thermal treatment, the following investigations of the system “coating-substrate” were made: adhesion, resistance to acids (H₂SO₄, HNO₃ and H₃PO₄ – concentration 60 %) and alkali NaOH. Phase composition, size of crystallites, morphology and elemental composition of the surface were analysed.

Given catalyst (large block) was assessed at temperature up to 600 °C, high gas flows $Q_{\text{gas}} = 2.75$ l/min and small oxygen amount $O_2 = 0.15$ %. The catalyst starts to operate at $T = 150$ °C–200 °C. Maximum conversion for CO = 80 % and NO_x = 100 % were obtained at 450 °C.

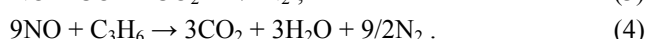
Given catalyst (small block) was assessed at temperatures up to 275 °C, low gas flows $Q_{\text{gas}} = 0.50$ l/min and large oxygen amount $O_2 = 20.0$ %. The catalyst (CO oxidation) started to operate at $T = 25$ °C, maximum conversion (100 %) was obtained at 240 °C.

Keywords: nanocrystalline, coatings, Co-Al-O, γ-Al₂O₃, adhesion, resistance to acids, X-ray diffraction, crystallite size, morphology, elemental composition, NO_x and CO catalysts.

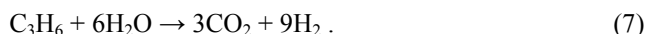
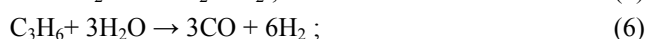
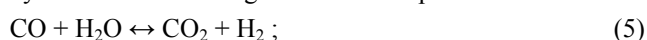
1. INTRODUCTION

A great concern over the role of nitrogen oxides, as one of the primary pollutants for the greenhouse effect, on ozone formation and depletion in stratosphere, on formation of photochemical smog, and acidic precipitation has received increasing attention since 1970s because of its harmful effect on life on earth in general. NO_x is produced by high temperature combustion of fossil fuels that use air as an oxidant, through endothermic oxidation of N₂ by O₂ [1]. Air pollution has emerged as a global problem and concentration of fine particles in the atmosphere has been shown to correlate with illness and mortality [2]. Research has shown that biodiesel-fueled engines produce less carbon monoxide (CO), unburned hydrocarbon (HC), and particulate emissions compared to mineral diesel fuel but higher NO_x emissions [3]. Three-way catalysts that control the pollutant emissions of HC, CO and NO_x are an effective way to reduce exhaust emissions [4].

The activity of three-way catalysts is highly dependent on the reactants present in the automobile exhaust gases (CO, NO_x, HC, O₂, H₂O, CO₂, and N₂) as well as their relative concentration. The overall catalytic reactions, which are important for controlling exhaust conditions, are given by the following equations [5]:



As well as the water–gas shift (WGS) and hydrocarbon reforming when water is present:



Similar reactions also occur in another fuel burning devices: domestic boilers, air heaters and etc. where catalysts could be used. Very important factor is that catalyst should begin to operate at as far as possible lower temperatures.

New technologies, incorporating the platinum group metals, are available to meet the exhaust emission regulations for cars, light duty and heavy duty vehicles and motorcycles being adopted by the European Union for implementation during the new century. These technologies include low light-off catalysts, more thermally-durable catalysts, improved substrate technology, hydrocarbon absorbers, DeNO_x catalyst and absorbers, selective catalytic reduction and diesel particulate filters. This large range of technologies will allow exhaust emissions from all engines, both on- and non-road, to be lowered to unprecedented levels [6].

However, catalyst produced using platinum group metals are very expensive, therefore it is trying to apply oxides of transition metals, putting additional requirements to substrates and coatings. The use of combustion catalysts can significantly lower the operating temperature. Indeed, the oxide of a metal such as cobalt, copper, or manganese, is active for the combustion of HC, CO, NO_x in the temperatures range 300 °C–600 °C [7].

The role of the support is to disperse the active phase. It must present good mechanical properties (resistance to attrition) and good thermal stability [8]. A very promising removal method of harmful NO_x emissions is the selective catalytic reduction (SCR). SCR can proceed efficiently with Co/SiO₂ and Co/Al₂O₃ catalysts if cobalt is well dispersed on the surface of the support [9].

Among these transition metal oxides, the cobalt oxide is one of the most versatile ceramic materials, since it is a p-type antiferromagnetic oxide semiconductor with the highest Curie temperature, $T_c = 1123$ °C. Cobalt forms two stable oxides: CoO and Co₃O₄, being Co₃O₄ the stable one

*Corresponding author. Tel.: +370-682-64883; fax: +370-37-323769.
E-mail address: arturasbabilius@gmail.com (A. Babilius)

at lower temperatures. Co_3O_4 has the normal spinel structure of the type AB_2O_4 , where Co^{2+} ions occupy the tetrahedral 8a sites and Co^{3+} occupy the octahedral 16d sites [10]. The cobalt oxide Co_3O_4 melting temperature is 1795°C , density 6450 kg/m^3 , crystalline structure – cubic, when cobalt/oxygen ratio is 73.4/26.6 (%). The high-valence cobalt oxides are thermally unstable and not commercially available on chemistry market. The CO oxidation activity decreases significantly with the oxidation state of cobalt, i. e., $\text{CoO} (+2) \geq \text{Co}_3\text{O}_4 (+8/3) \gg \text{CoO} (\text{OH}) (+3) \geq \text{CoO}_x (> +3)$ [11].

Co_3O_4 nanoparticles have various technical properties and potential applications in pigments (black nanometer pigment), coatings, catalysis, various types of sensors, anode materials in rechargeable batteries, solar energy absorbers, electro chromic, magnetism, etc [12].

Cobalt as element is also widely used in the Fischer-Tropsch catalysis (FT) [13]. Supported cobalt catalysts are preferred in FT synthesis of higher hydrocarbons from natural gas due to high activity and selectivity, low water-gas shift activity, resistance towards deactivation and comparatively low price. Unsupported cobalt oxide is very active species in the field of air pollution control of CO and NO_x and for the control of organic pollutants from effluent streams. Moreover, humidity-sensitive Co_3O_4 is active in the visible wavelength region at room temperature [14].

Nitric acid and nitrogen oxide have been produced using a Platinum/Rhodium catalyst. Cobalt oxide catalyst for ammonia oxidation reduces catalyst cost up to 75 %. Catalysts containing Co_3O_4 as the promoter display the lowest temperatures for 50 % conversion of methane, propane and propane [15].

Thin films of cobalt oxide have been prepared by various deposition techniques such as spray pyrolysis, sputtering, chemical vapor deposition (CVD), pulsed laser deposition, sol-gel process, electrophoresis deposition (EPD), etc., on a variety of substrates [10].

In this work we investigate the coatings obtained by the activated thermo-chemical condensate deposition (AT-CCD) method (system Co-Al-O). Adhesion, resistance to long-term chemical effect in alkalis and acids, phase composition, size of crystallites, morphology and chemical composition are analysed to study catalytic properties of the coatings and to find efficient conversion of carbon monoxide and nitrogen oxide when applying new designed catalytic converter.

2. EXPERIMENTAL

Catalytic coating (system Co-Al-O) of $30\text{ }\mu\text{m}$ thickness were formed on both sides of the substrate (strip steel 0C-404) of 40 micrometers thickness, by the AT-CCD method, without any additional preparation of the surface being coated, and without formation of any sublayer. Substrate temperature did not exceed 250°C during coating formation. AT-CCD method was analysed in previous authors publications and the details of experiment can be found in [16].

The coating was formed on ferritic stainless chromium steel 0C-404, which chemical composition is presented in the Table 1.

Table 1. Chemical composition of strip steel 0C-404 [17]

C	Cr	Al	Si	Mn	P	S
max			max	max	max	max
0.020	20.5	5.5	0.50	0.35	0.020	0.005

The system “coating–substrate” was analysed to define composition, morphology, mechanical, chemical and catalysts properties of Co-Al-O coatings [18].

The specimens were thermally treated in temperatures range from 100°C up to 1200°C . The heating rate of the specimens was 10°C/min . They were held in furnace for 4 hours. For the thermal treatment thermal furnace SNOL 1.6.1-11 was used.

Adhesion of the coatings (critical load) was determined by the “scratch” method – using a designed adhesion device [16].

The experiments of resistance to chemical effect in 60 % solutions of acid H_2SO_4 , HNO_3 , H_3PO_4 and alkali of NaOH were made using technically clean reagents.

Coating surface morphology and elemental composition of the coatings were investigated by SEM-EVO 50. Detector INCA_x was used for the EDS.

Phase identification was carried out using PDF-2 database [19], when X-ray diffractometer DRON-6 (Russia) with Cu K_α radiation was used in Bragg-Brentano geometry.

The crystallite size of the coating was determined by the Sherrer's equation and using X-fit program with pseudo Voight function modeling [20].

In order to make channels during its further fixing into cylinder-shaped roll (catalytic block), both sides of coated metal strip were corrugated (Fig. 1).

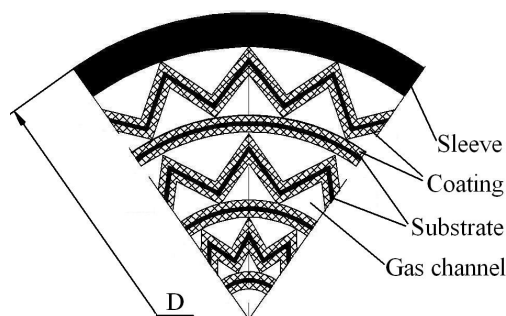


Fig. 1. Cross – section of the catalytic block

There were used two types: (a) and (b) catalysts blocks. Scrolled catalysts were put in thin stainless steel sleeves. The diameter of blocks (D), length of two blocks ($2L$), total geometric area of a catalytic wall (S), as well as volume (V) and test conditions of a block are following:

- Small block D-15: $D_{15} = 0.012\text{ m}$; $2L_{15} = 0.1\text{ m}$; $S_{15} = 0.12\text{ m}^2$; $V_{15} = 18\text{ cm}^3$. Gas parameters before blocks: $\text{O}_2 = 20\%$, $\text{CO} = 150\text{ ppm}$, $\text{NO}_x = 1\text{ ppm}$, $\text{CO}_2 = 0.2\%$, rate – $Q_g = 0.50\text{ l/min}$;
- Large block D-40: $D_{40} = 0.012\text{ m}$; $2L_{40} = 0.1\text{ m}$; $S_{40} = 0.40\text{ m}^2$; $V_{40} = 125\text{ cm}^3$. Gas parameters before blocks: $\text{O}_2 = 0.15\%$, $\text{CO} = 4000\text{ ppm}$, $\text{NO}_x = 40\text{ ppm}$, $\text{CO}_2 \sim 13\%$, rate – $Q_g = 2.75\text{ l/min}$.

In both cases scrolled catalysts were thermally treated at 700°C temperature at the rate of 10°C/min ., held for 4 hours and cooled with a furnace.

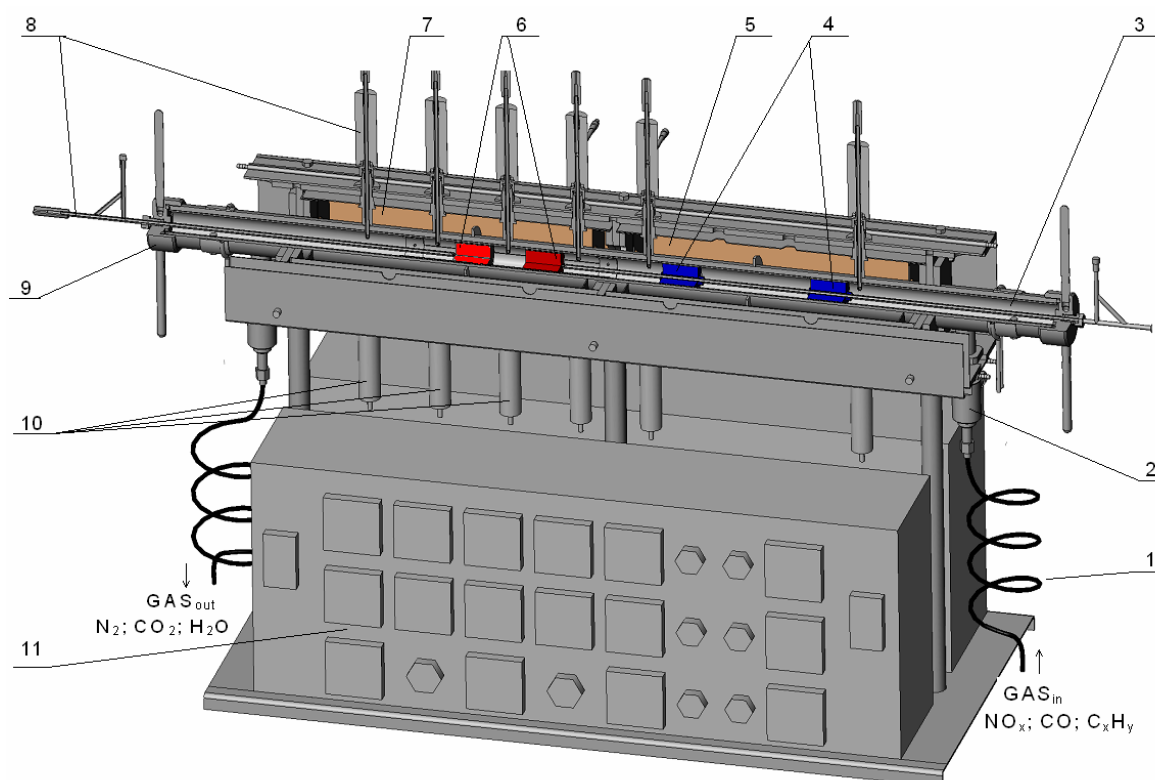


Fig. 2. Designed catalyst reactor: 1 – cooler, 2 – tube channel, 3 – reactor track, 4 – turbo blower, 5 – preheater, 6 – catalysts, 7 – heater, 8 – thermocouples of gas stream, 9 – stopper, 10 – thermocouples of reactor wall, 11 – electronic equipment (in colour on-line)

The analysis of incoming and outgoing gas from the catalysts reactor was made by gas analysers GreenLine 6000, Eurotron Instruments, Italy.

Catalyst experiments, for determining CO and NO_x conversion were made with a special design catalyst reactor (Fig. 2).

Heating temperature of the catalysts in converter during the experiment time was raised up to 275 °C for small blocks D-15 and up to 600 °C for large blocks D-40.

Operation of the catalyst converter is analysed below. Gas from the gas source through refrigerator “Gas_{in}” 1 and tube channel 2 flows to the catalyst reactor heated zone 3. There gas is mixed by a turbo blower 4 to have similar preheater’s 5 and heated gas temperature. Later gas accesses the catalyst blocks 6 where its chemical composition is changed. The catalyst blocks are heated by heaters 7. Gas temperature in full catalyst sector length is controlled by several thermocouples. After the gas flows from refrigerator “Gas_{out}” it is absorbed by a vacuum pump. Leakage in the reactor is secured by the stoppers 9. The monitoring of temperature of the reactor channel wall is performed by thermocouples 10. Gas chemical composition is constantly recorded by the gas analyser before and after catalyst block. In such way CO and NO_x conversion are calculated. The control of all parameters are performed with the electronic equipment 11.

3. RESULTS AND DISCUSSIONS

3.1. Composition, morphology and mechanical properties of Co-Al-O coatings

Coating adhesion (critical load) evaluated after the specimens were thermally treated at 100 °C was 25.0 N.

The increase of the treatment temperature up to 1100 °C gradually increased coating adhesion up to 48.2 N (Fig. 3).

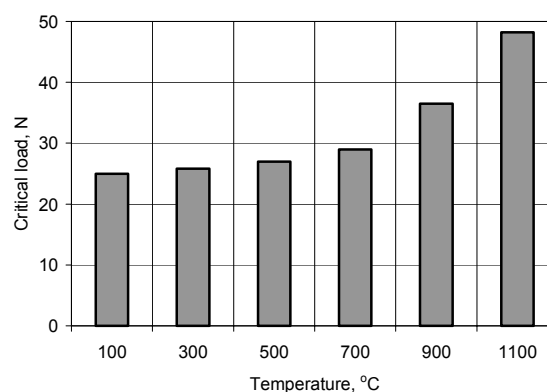


Fig. 3. Critical load of Co-Al-O coating (30 μm thick) in the scratch testing depending on thermal treatment temperature

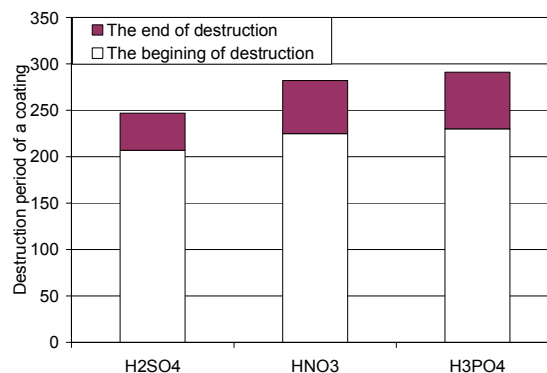


Fig. 4. Resistance of the system “coating–substrate” to 60 % acids H₂SO₄, HNO₃, H₃PO₄

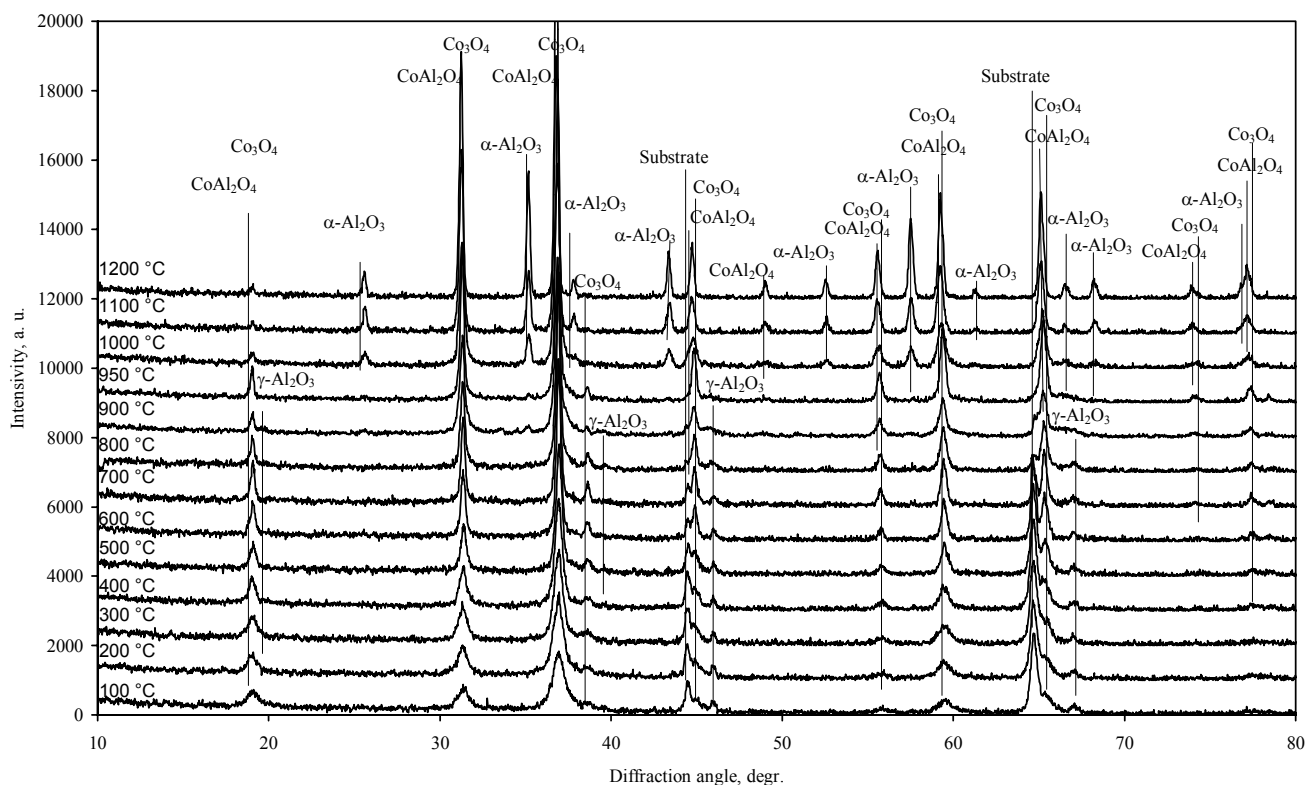


Fig. 5. X-ray diffraction patterns of a system “Co-Al-O coating – substrate”

Acids H_2SO_4 , HNO_3 and H_3PO_4 (concentration 60 %) fully destroyed system “coating – substrate” after 247, 281 and 292 hours accordingly (Fig. 4). Sudden loss of the specimens mass occurred when the substrate directly started to contact with acid solution.

1M and 5M NaOH solutions did not affect the system “coating – substrate” over 300 hours. This fact shows the inertness of the system “coating – substrate” to such kind of solution. High values of the coating adhesion, chemical resistance to the acids and alkalis show that the system (Co-Al-O) is stable enough mechanically and chemically.

XRD analysis showed that the system “coating – substrate” has five dominating phases: substrate metal phase Fe-Cr and oxide phases: $\gamma\text{-Al}_2\text{O}_3$, Co_3O_4 , CoAl_2O_4 and $\alpha\text{-Al}_2\text{O}_3$ (Fig. 5). There are no Al and Co phases in the coating. After thermal treatment in the temperature range 100 °C – 600 °C the coating was black colored. This is due to the high amount of Co_3O_4 phase in the coating. The black color is natural for phase Co_3O_4 at the temperature mentioned above. Due to the black color and high surface micro relief, Co-Al-O coating formed by the activated thermo-chemical condensate deposition method could be applied for the active elements of sun absorbers as well [12].

At higher temperatures purple color started to dominate. This is related with oxidation processes of coating and with the existence of new phases.

The crystallite size of the substrate (Fe-Cr phase) increased gradually from 40.2 nm to 99.1 nm at temperatures (200 °C – 700 °C). Temperature increase to 800 °C resulted in sudden increase of the crystallite size up to 257 nm (Fig. 6).

At temperature range from 100 °C up to 800 °C the $\gamma\text{-Al}_2\text{O}_3$ phase was detected. In this case crystallite size at

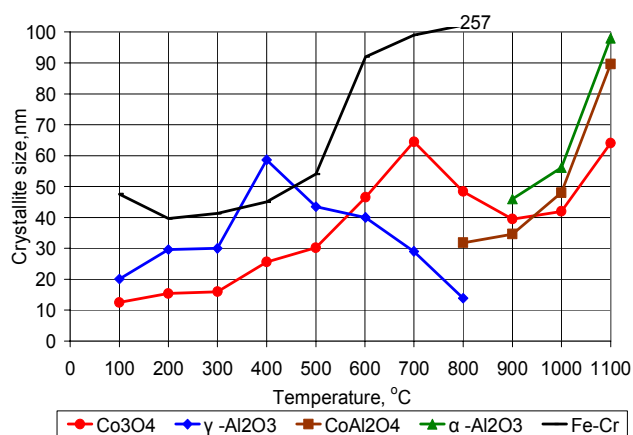
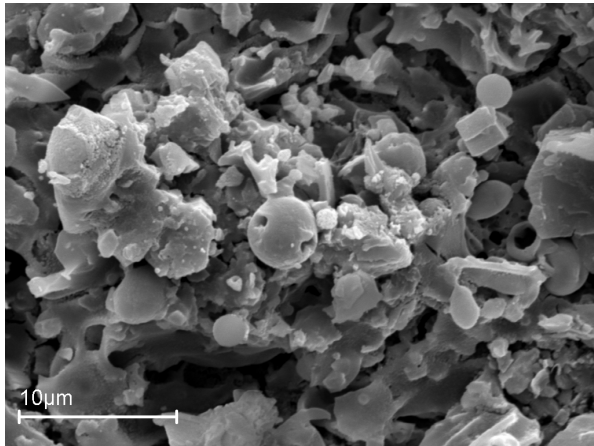


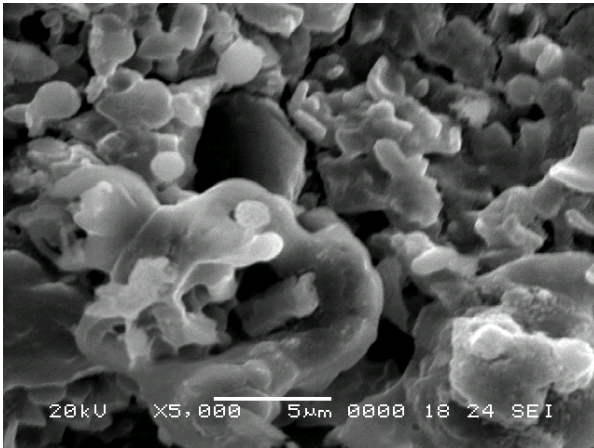
Fig. 6. The distribution of crystallite size of the system „Co-Al-O coating – substrate“

temperature 400 °C reaches its maximum value – 58.6 nm. Catalyst phase Co_3O_4 exists in the studied temperature range (from 100 °C to 1100 °C). The increase of temperature up to 1100 °C influences the crystallite size. The crystallite size varies from 12.5 nm to 64.8 nm and reaches maximum values at 700 °C and 1100 °C. According to [21, 22] crystallite size of Co_3O_4 powders can vary from 6 nm to 30 nm when it is heated up to 500 °C. This is in accordance with our performed experiments. However, information about Co_3O_4 crystallite size when the material is deposited onto metal substrate was not found. After thermal treatment, crystallite size of Co_3O_4 phase increases till the temperature 700 °C. The decrease of crystallite size when increasing thermal treatment temperature of the system “coating – substrate” is related with the appearance of new thermally stable phases CoAl_2O_4 and $\alpha\text{-Al}_2\text{O}_3$. Spinel phase CoAl_2O_4 appears at temperature 800 °C and

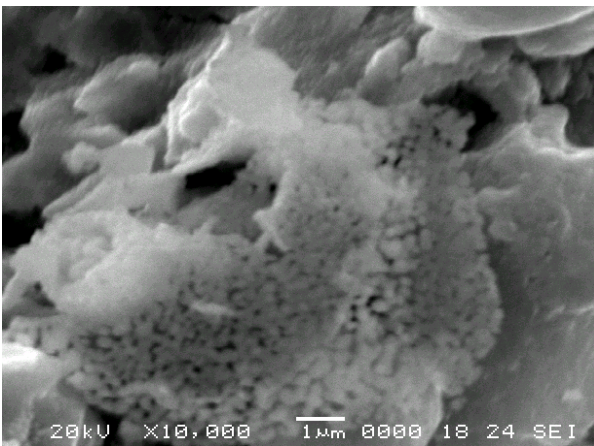
the crystallite size increases from 31.8 nm up to 89.7 nm with increasing temperature to 1100 °C. Corundum, α -Al₂O₃ phase starts at 900 °C and at temperature 1100 °C the crystallite size reaches 97.0 nm.



a



b



c

Fig. 7. Morphology of the Co-Al-O coating on a steel OC-404 plate after heat treatment at 700 °C

SEM picture (Fig. 7, a) illustrates morphology of the coating thermally treated at 700 °C temperature. At relatively lower magnification there is noticeable shape variety of single coating fragments. Figure 7, b, illustrates coating morphology at $\times 5000$ magnification, where sharply expressed macro relief is distinguished. The investigation

of topographical view of coating surface at $\times 10000$ magnification enables to detect coating fragments which occurs only in system Co-Al-O (Fig. 7, c). Coating surface was alloyed by ultra dispersive Co₃O₄ layer or derivatives of this oxide. This is in accordance with the results of elemental chemical composition defined from EDS spectra 2 (Table 3) and different locations of EDS spectra of coating (Fig.8).

It should be stressed that chemical composition of the substrate has affected the determination of coating surface elemental chemical composition. It is necessary to evaluate the fact, that the surface is porous and heterogeneous.

Distribution of the main chemical elements in the surface area of 10 mm² in mass units (%) measured using EDS is presented in the Table 2.

Table 2. Elemental chemical composition in the surface area of 10 mm² (from EDS spectra), %

C	O	Al	Cr	Fe	Co
2.26	28.26	20.14	3.31	8.78	37.26

Location of chemical composition of the coating surface in the area of 10 μm² – 50 μm² measured using EDS is presented in (Fig. 8), and the results in the Table 3. Five the most typical coating surface locations were analysed. Cobalt is one of the main elements in the coating.

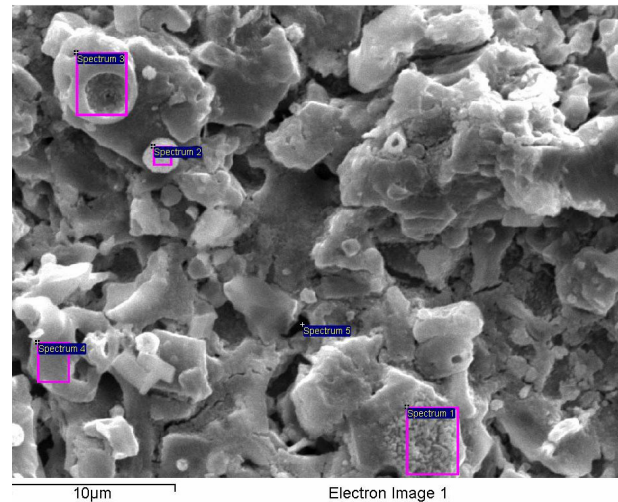


Fig. 8. Different locations (1, 2, 3, 4, 5) of EDS spectra of coating

Table 3. Elemental chemical composition at different locations of the coating surface (from EDS spectra)

Spectrum	Element, surface concentration, %					
	C	O	Al	Cr	Fe	Co
Spectrum1	1.65	27.50	21.71	1.33	1.32	46.49
Spectrum2	2.86	34.23	8.01	1.14	1.11	52.64
Spectrum3	3.73	41.24	36.72	0.45	0.81	17.05
Spectrum4	2.08	46.53	37.19	0.53	0.95	12.72
Spectrum5	0.21	4.45	3.01	15.11	53.32	23.91
Mean	2.11	30.79	21.33	3.71	11.50	30.56
Std.deviation	1.32	16.38	15.82	6.38	23.38	17.93
Max.	3.73	46.53	37.19	15.11	53.32	52.64
Min.	0.21	4.45	3.01	0.45	0.81	12.72

The fifth spectrum shows that the coating has cracks that continue almost up to the substrate surface. Moreover, variation of distribution of elemental chemical composition at different locations of coating is noticed.

3.2. Catalytic tests

3.2.1. CO and NO_x conversion at relatively high gas flow and small amount of oxygen (block D-40)

CO and NO_x conversion were investigated increasing catalyst block assessment temperature up to 600 °C (case, when oxygen quantity is relatively low) (Fig. 9). In the case of CO oxidation, the catalyst starts working at 150 °C, 50 % conversion is achieved at 310 °C, and maximum possible conversion – 80 % is achieved at 450 °C. In the case of NO_x reduction, the catalyst starts working at 200 °C, 50 % conversion is achieved at 330 °C, and maximum possible conversion – 100 % is achieved at 450 °C.

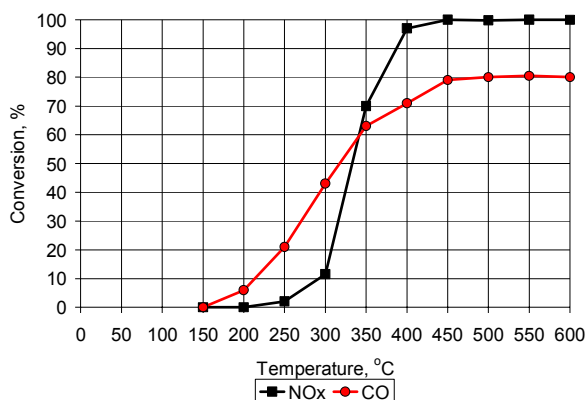


Fig. 9. Catalytic tests: block D-40. CO and NO_x conversion at relatively high gas flow and small amount of oxygen

3.2.2. CO conversion at relatively low gas flow and large amount of oxygen (block D-15)

The coatings formed by AT-CCD method showed good catalytic activity results according to CO conversion, when the oxygen amount at the entrance of catalyst converter was relatively high and gas flow – low. It is important to highlight, that the catalyst starts to work at $T = 25$ °C temperature. 50 % conversion was achieved at 110 °C, and full CO conversion to CO₂ was achieved at 240 °C (Fig. 10).

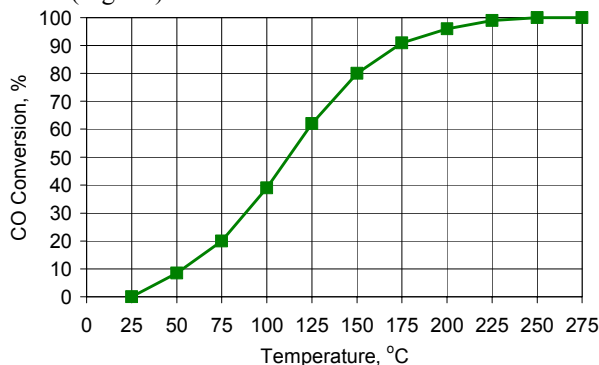


Fig. 10. Catalytic test: block D-15. CO conversion at relatively low gas flow and large amount of oxygen

4. CONCLUSIONS

1. Co-Al-O coating were deposited on substrate (steel OC-404) by the activated thermo-chemical condensate deposition method. Thermally treated in the temperature range 100 °C–1100 °C this “coating-substrate” system is long time resistant to 60 %: H₂SO₄, H₃PO₄ and HNO₃ solutions of acids. The system “coating- substrate” is inert to 1M and 5M of NaOH alkalis effects, performing experiments for 300 hours. Coating had good adhesion, critical load varied in a range 25 N–48 N.

2. All phases of coating are nanocrystalline. In the coating up to 800 °C catalytic carrier γ -Al₂O₃ phase (maximal crystallite size 58.6 nm) and catalytic active Co₃O₄ phase (maximum crystallite size 64.5 nm) exists in a whole temperature range 100 °C–1100 °C. Coating had structural defects, sharply expressed volatile relief. Approximate surface elemental chemical composition of the coating in mass units was as follow: Co – 37 %, Al –20 % and O – 28 %.

3. At relatively high gas flow $Q_{\text{gas}} = 2.75$ l/min and low oxygen amount – O₂ = 0.15 %, in case of CO oxidation the catalyst start working at 150 °C and maximum possible conversion 80 % was achieved at 450 °C. In case of NO_x reduction, the catalyst starts working at 200 °C and maximum possible conversion – 100 % was achieved at 450 °C.

At relatively low gas flow $Q_{\text{gas}} = 0.50$ l/min and high oxygen amount O₂ = 20.0 %, in case of CO oxidation, the catalyst starts working at 25 °C and maximum possible conversion – 100 % was achieved at 240 °C.

4. Co-Al-O coatings formed by the AT-CCD method could have practical application in the field of low temperature catalysts: automobile, boilers, domestic heating furnaces, gas – fire. The coatings are not expensive, are characterized with good technological reproduction of mechanical and catalytic properties.

REFERENCES

1. Xiong, W., Kale, G. M. High-selectivity Mixed-potential NO₂ Sensor Incorporating Au and CuO+CuCr₂O₄ Electrode Couple *Sensors and Actuators B* 119 2006: pp. 409–414.
2. Turrio-Baldassarria, L., Battistellia, C. L., Contia, L., Crebellia, R., Berardisa, B., Iamicelia, A. L., Gambinob, M., Iannaccone, S. Evaluation of Emission Toxicity of Urban Bus Engines: Compressed Natural Gas and Comparison with Liquid Fuels *Science of the Total Environment* 355 2006: pp. 64–77.
3. Agarwala, D., Sinhab, S., Agarwalb, A. K. Technical Note, Experimental Investigation of Control of NO_x Emissions in Biodiesel–Fueled Compression Ignition Engine *Renewable Energy* 31 2006: pp. 2356–2369.
4. Akcayola, M. A., Cinarb, C. Artificial Neural Network Based Modeling of Heated Catalytic Converter Performance *Applied Thermal Engineering* 25 2005: pp. 2341–2350.
5. Botas, J. A., Gutiérrez-Ortiz, M.A., González-Marcos, M. P., González-Marcos, J. A., González-Velasco, J. R. Kinetic Considerations of Three-way Catalysis in Automobile Exhaust Converters *Applied Catalysis B: Environmental* 32 2001: pp. 243–256.
6. Bosteel, D., Searles, R. A. Exhaust Emission Catalyst Technology. New Challenges and Opportunities in Europe *Platinum Metals Review* 1 (46) 2002: pp. 27–36.

7. **Fujita, S., Suzuki, K., Toshiaki, M.** Preparation of High-Performance Co_3O_4 Catalyst for Hydrocarbon Combustion from Co Containing Hydrogarnet *Catalysis Letters* 1 (86) 2003: pp. 139–144.
8. **Enache, D. I., Rebours, B., Roy Auberger, M., Revel, R.** XRD Study of the Influence of Thermal Treatment on the Characteristics and the Catalytic Properties of Cobalt–Based Fischer–Tropsch Catalysts *Journal of Catalysis* 205 2002: pp. 346–353.
9. **Stefanov, P., Anatasova, G., Marinova, T., Gomez-Garcia, J., Sanz, J. M., Caballero, A., Morales, J. J., Cordon, A., Gonzalez-Eliphe, A. R.** Characterization of Co/ZrO_2 De- NO_x Thin Film Catalysts Prepared by Magnetron Sputtering *Catalysis Letters* 3 (90) 2003: pp. 195–203.
10. **Apatiga, L. M., Castano, V. M.** Magnetic Behavior of Cobalt Oxide Films Prepared by Pulsed Liquid Injection Chemical Vapor Deposition from a Metal-organic Precursor *Thin Solid Films* 516 2008: pp. 1499–1502.
11. **Wang, C. B., Lin, H. K., Tang, C. W.** Thermal Characterization and Microstructure Change of Cobalt Oxide *Catalysis Letters* 1 (94) 2004: pp. 69–74.
12. **Mendoza, L., Albin, V., Cassir, M., Galtayrie, A.** Electrochemical Deposition of Co_3O_4 Thin Layers to Protect the Nickel–Based Molten Carbonate Fuel Cell Cathode *Journal of Electroanalytical Chemistry* 22 (548) 2003: pp. 95–107.
13. **Aaserud, C., Hilmen, A. M., Bergene, E., Eric, S., Shanke, D., Holmen, A.** Hydrogenation of Propane on Cobalt Fischer–Tropsch Catalysts *Catalysis Letters* 3 (94) 2004: pp. 171–176.
14. **Narayan, R. V., Kanniah, V., Dhathathreyan, A.** Tuning size and Catalytic Activity of Nano–Clusters of Cobalt Oxide *Journal of Chemical Sciences* 2 (118) 2006: pp. 179–184.
15. **Mellor, J. R., Palazov, A. N., Grigorova, B. S., Greling, J. F., Reddy, K., Letsoalo, M. P., Marsh J. H.** The Application of Supported Gold Catalysts to Automotive Pollution Abatement *Catalysis Today* 72 2002: pp. 145–156.
16. **Babilius, K., Babilius, A.** Research of Coatings Obtained in the Activated Thermo-Chemical Condensate Deposition Method, Al-O System *ISSN 1392-1320 Materials Science (Medžiagotyra)* 12 (2) 2006: pp. 114–119.
17. [http://www2.sandvik.com/sandvik/0140/internet/se01596.nsf/GenerateFrameset1?readForm&url=http://www2.sandvik.com/sandvik/0140/internet/se01596.nsf/\(DocumentsInternetWeb\)/FB66C1416B15E96C41256713003A4C3A](http://www2.sandvik.com/sandvik/0140/internet/se01596.nsf/GenerateFrameset1?readForm&url=http://www2.sandvik.com/sandvik/0140/internet/se01596.nsf/(DocumentsInternetWeb)/FB66C1416B15E96C41256713003A4C3A)
18. **Babilius, K., Babilius, A.** Cu-Al-O System: Catalytic Coatings Obtained by the Activated Thermo-chemical Condensate Deposition Method *ISSN 1392-1320 Materials Science (Medžiagotyra)* 14 (1) 2008: pp. 23–28.
19. JSPDS Cards – International Center for Diffraction Data. 12 Campus Boulevard Newtown Square, PA 19073–3273 USA.
20. **Cheary, R. W., Coelho, A. A.** (1996). Programs XFIT and FOURYA, deposited in CCP14 Powder Diffraction Library, Engineering and Physical Sciences Research Council, Daresbury Laboratory, Warrington, England. (<http://www.ccp14.ac.uk/tutorial/xfit-95/xfit.htm>).
21. **Lendzio-Bielun, Z., Podsiadly, M., Narkiewicz, U., Arabczyk, W.** Effect of Structural Promoters on The Reduction Process of Nanocrystalline Cobalt *Reviews on Advanced Materials Science* 12 2006: pp. 145–149.
22. **Khodakov, A. Y.** Enhancing Cobalt Dispersion in Supported Fischer–Tropsch Catalysts Via Controlled Decomposition of Cobalt Precursors *Brazilian Journal of Physics* 39 (1A) 2009: pp. 171–175.